Conformational Change of Giant DNA with Added Salt As Revealed by Single Molecular Observation

Naoko Makita,[†] Magnus Ullner,[‡] and Kenichi Yoshikawa*[,§]

Faculty of Environmental and Information Sciences, Yokkaichi University, Yokkaichi 512-8512, Japan; Theoretical Chemistry, Center for Chemistry and Chemical Engineering, Lund University, P.O. Box 124, SE-221 00 Lund, Sweden; and Department of Physics, Graduate School of Science, Kyoto University, Kyoto 606-8502, Japan

Received March 24, 2006; Revised Manuscript Received July 11, 2006

ABSTRACT: The structural change of individual giant double-stranded T4 DNA (165.6 kilobase pairs) molecules as a function of salt concentration was investigated by single molecular observation with fluorescence microscopy in a wide range of concentration of NaCl, 1×10^{-6}−3 M. The measured long-axis length was transformed into a persistence length and subjected to a power-law analysis, which showed that the electrostatic contribution to the persistence length is inversely proportional to the square root of the salt concentration; i.e., it has a linear dependence on the screening length. This is interpreted as the behavior of a flexible chain with electrostatic excluded-volume interactions. Although double-stranded DNA is locally stiff, it displays flexibility when the contour length is much longer than the persistence length, as is the case for T4 DNA.

1. Introduction

Since the discovery of the double-stranded structure of DNA more than half a century ago, the structure of DNA has been actively studied in relation to its genetic functions. It has been well established that the double-stranded DNA is rather stiff, with a persistence length on the order of 50 nm and a thickness of 2 nm.[1−4] This implies a rodlike character for short DNA. On the other hand, genomic DNA molecules are rather long; they are millimeter scale in prokaryotes and centimeter scale in eukaryotes. These giant DNA molecules behave as a semiflexible polymer chain and take a random-coil state in aqueous solutions. Despite the well-established knowledge on short DNAs, the conformational characteristics of these giant DNAs have not yet been fully clarified. This may be largely due to the experimental difficulties when treating giant DNA molecules, with a constant risk of cutting the chain. Even a small mechanical agitation induces the breakage of giant DNA into fragments. Thus, it is necessary to establish new methodologies in order to shed light on the conformational behavior of giant DNAs.

About a decade ago, by using the experimental technology of single DNA observation, it was found that giant DNA molecules undergo large discrete transition between elongated coil state and folded compact state.[5−11] On the other hand, the ensemble of giant DNAs always exhibit continuous transition because of the rather wide region of the coexistence of the coil and compact states. In the present study, we have focused our interest on the conformational characteristics of giant DNA in a random-coil state with special attention to the salt effect.

There is also a long history of theoretical studies aimed at the conformational behavior of polyelectrolyte molecules and their salt dependence.[12] It has been particularly popular to predict the persistence length due to the electrostatic interactions. One reason for this is that Odijk[13] and Skolnick and Fixman[14] (OSF) found a simple power law for the electrostatic persistence length when analyzing the bending energy of rodlike molecules. As a result, much of the subsequent discussion about persistence length, including experimental findings, has been focused on the existence and form of a power law. Our data will also be put into this framework.

A general problem in discussions of persistence length is that it is not a single, unique property. In fact, there are no fewer than four different definitions of persistence length.[15] They are all equivalent for the wormlike-chain model, but not if different parts of the chain can interact and especially not with long-ranged electrostatic interactions. While theory can adopt any of the definitions, which has caused considerable confusion in the past,[15−17] experimental approaches have at least been consistent. Since the persistence length is not measured directly, the experimental observable has to be converted with the help of a model, and the natural choice is the wormlike chain. The calculation of a measurable quantity within the framework of the wormlike chain generally involves an integration over the orientational correlation function, which means that the persistence length obtained by comparison with the model calculation is a projection length. Projection length is a name given to one of the four definitions to semantically separate it from the other three.[15] It is actually a group of definitions, characterized by the integration over the orientational correlation function. If the integral is not weighted, it corresponds to the projection of the end-to-end vector on the direction of the first bond. Other quantities, such as the radius of gyration, are obtained from a weighted integral, but simulations have shown that different ways to calculate projection length leads to the same qualitative results.[16]

The advantage of projection length is that it offers a consistent means to compare different types of conformational investigations, such as light scattering and viscosity studies. It is important to note, however, that it is obtained from global quantities, and it would be a mistake to try to interpret the projection length as a representation of the local chain behavior. This is also the reason why the wormlike chain model can be

[†] Yokkaichi University.
[‡] Lund University.
[§] Kyoto University.
* Corresponding author: e-mail yoshikaw@scphys.kyoto-u.ac.jp.

10.1021/ma060669b CCC: $33.50
Published on Web 08/11/2006

used, despite the fact that real molecules are not wormlike, especially not polyelectrolytes. In the experimental context, projection length should be regarded as an operational definition.

Experimental investigations of how the persistence length (or a convertible quantity, such as radius of gyration) changes with added salt can be divided into two groups. Stiff molecules, such as DNA, show agreement with OSF theory,[18−20] which may be expressed as a quadratic dependence on the Debye screening length. Flexible molecules, on the other hand, yield an electrostatic contribution to the persistence length that is linear in the screening length.[21−26] The latter result has also been the conclusion of many simulations measuring the projection length.[15,16,27−29] More recent simulations have shown that the linear dependence is coupled to excluded-volume effects,[17,30,31] i.e., the effects of the chain being able to bend back on itself, causing occasional interactions between distant parts of the chain. On the scale of the conformational fluctuations, these interactions may be treated as short-ranged and on average be represented by a localized volume, which is how excluded-volume theory treats interactions. On the other hand, on the local scale along the chain, electrostatic interactions may still be long-ranged in the sense that they cover several monomeric units.

There have been attempts to include an excluded-volume treatment into the analysis of the experimental results. In light scattering experiments, "corrected" persistence lengths have been obtained through excluded-volume theory without explicit consideration of electrostatic interactions by using the measured second virial coefficient to extract an underlying wormlike chain from the radius of gyration[32] or fitting the intramolecular scattering function to a theoretical expression for a wormlike chain with excluded-volume effects.[3,33,34]

Electrostatic interactions have been included by combining OSF theory with excluded-volume theory,[22,23,25−27,35] as originally suggested by Odijk and Houwaart.[36] Knowing the relevant parameters makes it possible to calculate the radius of gyration directly without fitting and compare it to the experiments. The latter approach has also been tested by simulations,[27,37,38] which show similar trends in the comparison as the experimental results. Although it is possible to get decent agreement with parameters obtained independently, the connection to the local chain behavior is still not completely understood. While the Odijk−Houwaart approach allows for the conceptual separation of long-range electrostatic interactions along the chain and an excluded-volume treatment on a larger scale, it is still subject to the OSF requirement that the molecule is intrinsically stiff, which has been analyzed by Barrat and Joanny.[39] Simulations of flexible molecules have shown that, by removing the excluded-volume interactions in a regime where they would otherwise be present, the chain behavior does not agree with the OSF result.[17] In other words, the Odijk−Houwaart approach does not work as a general explanation for deviations from the OSF prediction.

The radius of gyration of somewhat hydrophobic polyelectrolytes has been well fitted[40] by the theory of Muthukumar,[41,42] which follows in the tradition of variational calculations based on the freely jointed chain, first applied to polyelectrolytes by Kuhn, Künzle, and Katchalsky.[43,44] In its simplest form, this type of calculation is known as the Flory approach.[45,46] Even more advanced variational calculations based on the freely jointed chain and screened Coulomb interactions tend to give the same result as the Flory approach for the projection length,[17] i.e., a linear dependence on screening length in the absence of excluded-volume effects or a weaker dependence with a power law exponent of 0.8 instead of 1 when the screened Coulomb interactions are treated as a localized volume as in traditional excluded-volume theory. The theory of Muthukumar retains a more complex form, but in the limit of a chain extended only by screened Coulomb interactions it also gives the latter result. This is in line with the experimental results of Beer et al.,[40] who see a weaker dependence on the screening length for their hydrophobic polyelectrolytes than usually reported, with exponents corresponding to powers between 0.6 and 0.96. However, if we accept a power of 1 as the general result for polyelectrolytes without hydrophobic interactions, as seen in experiments and simulations, and that this is a result of excluded-volume effects, the conclusion is that variational calculations based on the freely jointed chain give the correct behavior in the absence of the central effect, while as an excluded-volume treatment, they give a slightly weaker dependence on the screening length, at least in the Flory limit. A problem with most theories is that they end up using a single parameter to describe the conformational behavior on all length scales, which is acceptable in the rod limit but not for flexible polyelectrolytes.[17] The limitations of the usual variational approach have also been discussed by Manghi and Netz.[47] Beer et al. also tested the Odijk−Houwaart approach in an appendix and concluded that the fit was good, but for unrealistic parameters.

In other words, the theoretical treatment of excluded-volume effects is a complex matter that needs to be studied carefully, and we will not venture further into this discussion here. The operationally defined projection length, as discussed above, is more straightforward and sufficient for comparing our results with previous investigations.

The purpose of the present study is to examine the salt effect on the conformational behavior of giant DNA with a number of segments well above 100 kilobase pairs (kbp). Here the focus is on T4 DNA as a very large polyelectrolyte. However, in the long run, we expect that unraveling the fundamental physicochemical properties of giant DNA will contribute to an understanding of the relationship between the structure and function of genomic DNA, although the results presented here only represent a small step in that direction.

2. Methods

2.1. Sample Preparation. The DNA used was bacteriophage T4 DNA (165.6 kbp, Nippon Gene), dissolved in an aqueous solution with a fluorescent dye, at various concentrations of NaCl (1×10^{-6}−3 M). The dyes used were DAPI (4,6-diamidino-2-phenylindole, Wako Pure Chemical Industries, Ltd.) and YOYO-1 (quinolinium, 1,1′-[1,3-propanediylbis[(dimethyliminio)-3,1-propanediyl]]bis[4-[(3-methyl-2(3*H*)-benzoxazolylidene)methyl]]-, tetraiodide, Molecular Probes, Inc.). DAPI can be used for DNA observation even at extremely high concentrations of salt, but we could not observe DNA molecules with DAPI at salt concentrations below 10^{-4} M. YOYO-1, on the other hand, enabled the low-salt observations but could not visualize DNA at the higher salt concentrations.

For one set spanning higher concentrations of NaCl (1×10^{-4}−3 M), DNA was diluted to a final concentration of 100 nM in nucleotides and stained with 100 nM DAPI. The DNA solutions were gently mixed and observed after 10 min. For the other set with lower salt concentrations (1×10^{-6}−1×10^{-2} M), the final concentration of DNA was designed to be extremely dilute, 1 nM in nucleotides, to prevent overlapping of DNA molecules, as they were several times more extended at conditions of low salt than at high. Here we used 0.1 nM YOYO-1 instead of DAPI. YOYO-1-stained DNA samples were prepared by diluting the stock solution with aqueous NaCl solutions or Milli-Q water and were observed after 10 min. The composition of the stock solution, which was

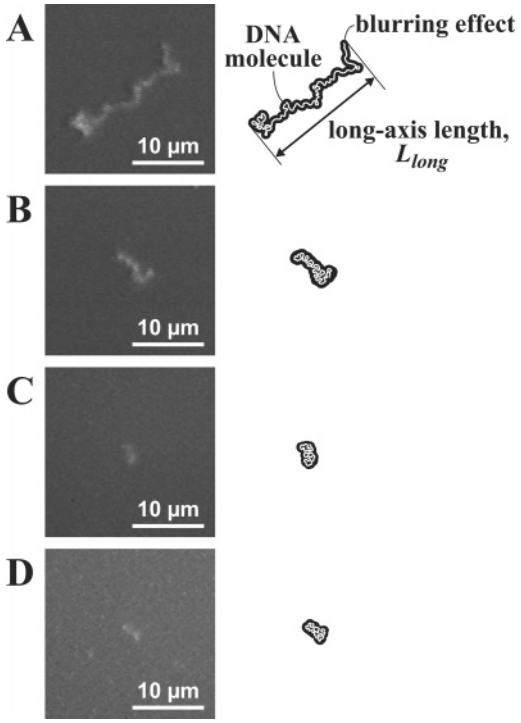

Figure 1. Fluorescence images of single T4 DNA molecules in the bulk solutions at (A) 1 μM, (B) 100 μM, (C) 10 mM, and (D) 3 M NaCl (left panel). Schematic representations of the conformation of the DNA molecules (right panel). The fluorescent dyes used to stain DNA are YOYO-1 (A, B) and DAPI (C, D).

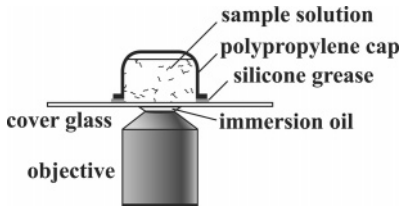

Figure 2. Schematic diagram of the experimental setup. The solution depth is about 5 mm.

allowed to equilibrate for at least 12 h at 4 °C, was 100 nM T4 DNA in nucleotides, 10 nM YOYO-1, and 1×10^{-5} M NaCl.

2.2. Fluorescence Microscopic Observation. Single DNA molecules were observed by fluorescence microscopy (FM) using a Carl Zeiss microscope, Axiovert 135 TV, equipped with a high-magnification (100×) or a low-magnification (40×) oil-immersion objective. The 100× objective was mainly applied to detailed observations of the relatively compact DNA molecules at the higher salt concentrations, whereas we predominantly used the 40× objective in order to capture the whole conformation in a clear manner for the more extended DNA molecules at low salt concentrations.

Real-time fluorescence images were recorded on videotape through a highly sensitive Hamamatsu EB-CCD camera and an image processor Argus 10 (Hamamatsu Photonics). Because of the relatively low time resolution and high sensitivity of the camera, the Brownian motion leads to a blurring effect, as is schematically shown in Figure 1.[5] FM observations of DNA free in solution were carried out at room temperature (21 ± 1 °C). By putting a large quantity of sample solution on the glass, as shown in Figure 2, we could make the bulk conditions independent of the surface, and to avoid direct interactions, DNA was measured at least 50 μm away from the surface. To clean the surface, the glass microscope slides were baked in an electric oven for 1 h at 500 °C before observation. It was found that DNA never attached to the glass surface when using this procedure. After acquiring DNA images, they were analyzed with a Cosmos image processor (Library Inc.). The long-axis length, L_{long}, defined as the longest distance in the outline of a DNA image (Figure 1), was measured on 50 randomly chosen DNA molecules under fixed conditions, which also meant a random sampling of three-dimensional orientations, projected onto the two dimensions of the image.

To confirm the contour length of DNA molecules at each salt concentration, individual DNAs were attached to a silanized glass surface and stretched by flow. The silanization of the glass was performed as follows. The baked glass was soaked in 1% (v/v) *N*-trimethoxysilylpropyl-*N*,*N*,*N*-trimethylammonium chloride in methanol at room temperature for 1 h, washed with methanol, and baked in an electric oven for 2 h at 120 °C.

2.3. Monte Carlo Simulations. Chains with 1000 monomers joined by 0.3 nm long rigid bonds were simulated using the traditional Metropolis algorithm[48] to investigate correlations between the long-axis length and other conformational parameters. Three different models were used: a freely jointed chain, a freely rotating chain with fixed bond angles, and a charged freely jointed chain. The conformational sampling was performed with a pivot algorithm,[49,50] where trial conformations were obtained by dividing the chain into two parts around a randomly chosen bond. All monomers on one side of the bond were given a random rotation within a full circle with the bond as the rotation axis for the freely rotating chains and with a random rotation axis for the freely jointed chains.

In the charged chains, the monomers interacted through a screened Coulomb potential

$$u_{sc}(r) = \alpha^2 k_B T l_B \frac{e^{-\kappa r}}{r} \tag{1}$$

where α is the degree of ionization of a charged site, k_B Boltzmann's constant, and T is the temperature. $l_B = e^2/(4\pi\epsilon_r\epsilon_0 k_B T)$ is the Bjerrum length, with e being the elementary charge, ϵ_r the dielectric constant of the solution, and ϵ_0 the permittivity of vacuum. When the polyelectrolyte is infinitely diluted and only monovalent ions are present, the ionic strength can be expressed as the concentration, C_s, of added 1:1 salt, and the Debye screening parameter can be written as

$$\kappa^2 = 8\pi l_B N_A C_s \tag{2}$$

where N_A is Avogadro's number. κ^{-1} is known as the screening length and represents the range of the (screened) electrostatic interactions. The simulations were performed with $\alpha = 1$, $T = 298$ K, and a dielectric constant $\epsilon_r = 78.3$ corresponding to water at room temperature, which gives $l_B \approx 0.716$ nm. The screening parameter is expressed in terms of concentration of added salt through eq 2, and values in the range $C_s = 0-0.1$ M were simulated.

The long-axis length, L_{long}, was sampled by projecting a conformation on a randomly oriented plane and finding the largest monomer−monomer separation on the plane. The radius of gyration, R_G, was calculated according to its definition:

$$R_G^2 = \frac{1}{N}\sum_{i=1}^{N}\langle(\mathbf{x}_i - \mathbf{x}_{cm})^2\rangle \tag{3}$$

where N is the number of monomers, $\mathbf{x}_i$ and $\mathbf{x}_{cm}$ are the coordinates of monomer i and the center of mass, respectively, and $\langle ... \rangle$ denotes an ensemble average. The long-axis length and the radius of gyration were averaged over simulations with 5×10^7 pivot moves for charged chains and 5 times longer for uncharged chains (because the latter simulations were so quick anyway) after equilibration for 5×10^4 and 1×10^5 pivot moves, respectively.

3. Results

Figure 1 shows the fluorescence images of DNA molecules at different concentrations of NaCl. At the lowest salt concentration (1 μM NaCl, Figure 1A), DNA molecules take expanded conformations. With an increase in the salt concentration, the

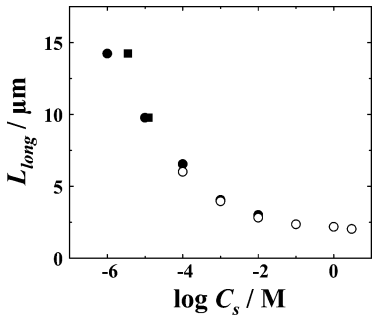

Figure 3. Long-axis length as a function of the concentration of added NaCl using YOYO-1 (filled circles) and DAPI (open circles). Also shown are values shifted to correspond to the ionic strength assuming a pH of 5.6 (filled squares).

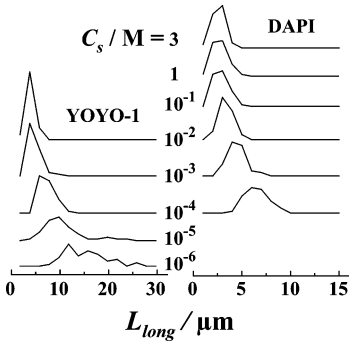

Figure 4. Distribution of long-axis length at various concentrations of added NaCl. Each point for YOYO-1 (left panel) and DAPI (right panel) represents a data interval of 2 and 1 μm, respectively.

conformations tend to shrink and become more dense. As mentioned above, we used two fluorescent dyes, DAPI and YOYO-1. DAPI binds to DNA in the minor groove and is known to have a minimal effect on the DNA conformations, whereas intercalators such as YOYO-1 increase the contour length.[51] In the present study the longest contour lengths of DNA with DAPI and YOYO-1 were 58 and 65 μm, respectively, which may be compared to 56 μm calculated from the helical rise of canonical B-DNA, 0.34 nm.[52−54] The previous measurements of the contour length of T4 DNA with DAPI produced a maximum value of 57 μm,[51] in close agreement with our result.

The results for the long-axis length, L_{long}, at different concentrations of NaCl are given in Table 1. The average values of L_{long} are also plotted in Figure 3. Figure 4 shows the measured distributions. The results were obtained from measurements of 50 molecules at each condition, which means that the estimated standard deviation of the mean value of L_{long} is a factor of $\sqrt{50} \approx 7.1$ smaller than the standard deviation obtained for the distribution, which is given in Table 1. With an increase in the concentration of NaCl, the spatial extension of DNA decreases. However, beyond the physiological salt concentrations, above 100 mM, the spatial size of DNA does not show significant change; i.e., in this region the salt effect on the extensity of DNA becomes "saturated". At intermediate salt concentrations, 0.1−10 mM NaCl, we observed DNA molecules using both DAPI and YOYO-1. In each case, the value of L_{long} with YOYO-1 was a bit larger than with DAPI, which probably reflects the increased contour length caused by the intercalator. At the lower salt concentrations, the width of the L_{long} distribution tends to increase.

Figure 5 shows the results of the time trace and the distribution of L_{long} for a single DNA molecule at two concentrations of NaCl, 1 μM and 1 M. The time averages of L_{long} are 14.38 and 2.20 μm, respectively. The standard

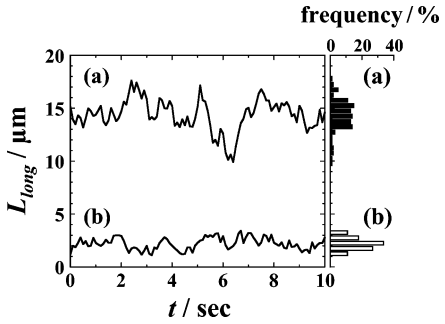

Figure 5. Time traces of the long-axis length of T4 DNA molecules together with the data collected as a histogram for (a) 1 μM and (b) 1 M NaCl solutions. The time interval is 1/10 s.

Table 1. Long-Axis Length, L_{long}, with the Standard Deviation of the Distribution in Parentheses and Persistence Length, l_p, at Different Concentrations, C_s, of Added NaCl for Measurements with YOYO-1 and DAPI as the Fluorescent Probe

	L_{long}/μm		l_p/nm	
C_s/M	YOYO-1	DAPI	YOYO-1	DAPI
1×10^{-6}	14.23 (4.15)		1609	
1×10^{-5}	9.78 (4.19)		730	
1×10^{-4}	6.55 (1.37)	6.02 (1.17)	321	304
1×10^{-3}	4.06 (1.30)	3.96 (0.924)	122	131
1×10^{-2}	3.02 (0.919)	2.83 (0.720)	67.6	66.5
1×10^{-1}		2.37 (0.772)		46.6
1×10^{0}		2.19 (0.727)		39.8
3×10^{0}		2.04 (0.588)		34.5

deviations based on 100 data points from each time trace shown in the figure are 1.49 and 0.564 μm, respectively, indicating that the time-dependent fluctuation, i.e., the intrachain Brownian motion, is significantly larger for the specimen at the lower salt concentration.

4. Discussion

4.1. Caveats for Low Ionic Strengths. The measurements at the lowest ionic strengths are associated with a number of uncertainties, beside the large conformational fluctuations. Since no buffer is added in the preparation of the stock solution or samples, CO_2 from the air is likely to acidify the solution. A rough estimate for a solution fully equilibrated with CO_2 from the air at normal conditions yields a pH around 5.6, corresponding to an ionic strength on par with the smallest additions of NaCl. The filled squares in Figure 3 show how the results shift if this pH is included in the ionic strength (treated as extra added salt). Considering the small volume of the sample under the microscope, saturation by CO_2 is feasible but not guaranteed. Leakage of sodium ions from the glassware may also contribute to the ionic strength at the lowest NaCl concentrations, while ionic species from the DNA stock solution are so dilute that they can be ignored.

There are also questions about the state of DNA itself. For salt-free DNA solutions, denaturation has been found to occur at DNA concentrations on the order of 10^{-4} M.[55−58] At these concentrations, DNA can be stabilized by about 10^{-4} M salt.[57,58] Thus, in our case, where the DNA concentrations are lower, we could expect some denaturation to occur at least below 10^{-4} M concentrations of added NaCl. On the other hand, the dye, which binds to DNA, may counteract the denaturation, especially YOYO-1 used at the lowest salt concentrations, which is an intercalator. No direct evidence of denaturation was observed, although there could still be limited local tendencies.

These considerations suggest that the results for the lowest ionic strengths should be taken with a grain of salt.

Table 2. Ratio between the Radius of Gyration and the Long-Axis Length, R_G/L_{long}, in Simulations with Resulting Shape Factors, R_{ee}^2/R_G^2, Ranging from 6 (Freely Jointed Chain) to 12 (Rigid Rod)[a]

R_{ee}^2/R_G^2	R_G/L_{long}	γ (deg)	α	C_s/M
6.0	0.36	90	0	
6.0	0.37	140	0	
6.2	0.39	160	0	
6.4	0.40	167	0	
6.6	0.40	130	1	0.1
7.2	0.41	172	0	
7.7	0.41	139	1	0.01
8.6	0.41	175	0	
10.5	0.39	144	1	0.001
11.7	0.37	150	1	0.0
12.0	0.37	180	0	

[a] Apart from the case with the bond angle $\gamma = 90°$, which is the result for a freely jointed chain, the simulation results are either for uncharged chains ($\alpha = 0$) with fixed bond angles or charged chains ($\alpha = 1$) with screened Coulomb interactions corresponding to salt concentrations, C_s, ranging from 0 to 0.1 M. For the freely jointed chain and the charged chains, γ is the average bond angle. The rigid-rod result was obtained analytically. The chains were composed of 1000 monomers with bond lengths of 0.3 nm.

4.2. Conformational Behavior. In the experiments, we have measured the long-axis length, L_{long}, in a two-dimensional projection. To make the results comparable to theory and experiments in general, we need to establish a connection to more common conformational measures, such as end-to-end distance, R_{ee}, and radius of gyration, R_G. It might be tempting to equate the long-axis length with a projection of the end-to-end distance, but for a flexible chain, the longest intramolecular distance is not necessarily between the ends.

We have performed a series of simulations of chains with a large range of stiffness, from freely jointed chains to nearly rodlike, and calculated the average values of the different conformational measures in each case. It turns out that the long-axis length measured on an arbitrary plane is strongly correlated to the radius of gyration with a ratio R_G/L_{long} of about 0.4 (see Table 2).

Note that the internal behavior of the charged chains is rather complex with several relevant length scales, but the overall behavior reflected by the ratio of global quantities, such as R_G and L_{long}, is consistent with the simpler models. The results are therefore assumed to be model independent and also applicable to DNA.

The radius of gyration can be related to a persistence length, l_p, via the expression for a wormlike chain

$$R_G^2 = \frac{l_p L}{3} - l_p^2 + 2\frac{l_p^3}{L} - 2\frac{l_p^4}{L^2}(1 - e^{-L/l_p}) \qquad (4)$$

which for very long chains ($L \gg l_p$) becomes

$$R_G^2 = \frac{l_p L}{3} \qquad (5)$$

Thus, using the proportionality between L_{long} and R_G, the former can be transformed into a persistence length by rearranging eq 4 and solving for l_p iteratively. As was discussed in the Introduction, the result is a projection length, which should not be confused with any of the other three basic definitions of persistence length.[15] In particular, the fact that the wormlike-chain model has been used does not mean that the DNA molecule can be regarded as wormlike. On the contrary, the projection length includes the deviations from that behavior. The point of the procedure is that it makes our results comparable to other experiments where a global quantity has been transformed into a persistence length using an expression obtained for a wormlike chain, which is a very common approach. The results also become comparable to simulation studies reporting the projection length.

The calculation of l_p requires a known contour length, and we used the observed values of 58 and 65 μm for measurements with DAPI and YOYO-1, respectively. The difference in contour lengths compensates for the systematic differences in long-axis length and, unlike the latter, the persistence length is not consistently larger for YOYO-1 compared to DAPI, as can be seen in Table 1.

In the theory of Odijk[13] and Skolnick and Fixman[14] (OSF), the total persistence length may be expressed as the sum of an intrinsic part and an electrostatic part

$$l_p = l_{p,0} + l_{p,e} \qquad (6)$$

For very long chains, they obtained

$$l_{p,e} = \frac{\alpha^2 l_B}{4\kappa^2 b^2} \qquad (7)$$

where b is the contour distance between neighboring sites. We can express the OSF result as the electrostatic persistence length depending quadratically on the screening length or, equivalently, given eq 2, being inversely proportional to the salt concentration.

The behavior predicted by OSF theory has been observed for rather stiff molecules,[18−20] with DNA being a typical example. However, the big question has been if it also applies to flexible chains. Experiments have reported electrostatic persistence lengths with a linear dependence on the screening length,[21−26] instead of the quadratic behavior of OSF theory. This has also been the conclusion of many simulations measuring the projection length.[15,16,27−29] More recent simulations have shown that the linear dependence is coupled to excluded-volume effects,[17,30,31] i.e., the effects of the chain being able to bend back on itself, causing occasional interactions between distant parts of the chain.

Thus, the next step is to investigate if the persistence length displays a power-law behavior with respect to the salt concentration. If we say that the projection length consists of an intrinsic part, $l_{p,0}$, independent of the ionic strength, and an electrostatic part with a power-law dependence on the salt concentration, C_s, it can be written as

$$l_p = l_{p,0} + \frac{A}{C_s^w} \qquad (8)$$

where A contains the dependence on the other system parameters. Note that the second term in eq 8 contains all deviations from the intrinsic behavior, including excluded-volume effects, which also have an electrostatic component. By plotting $\log(l_p - l_{p,0})$ vs $\log C_s$, we get the power w, while l_p vs C_s^{-w} can be extrapolated to to yield $l_{p,0}$ at $C_s^{-w} = 0$. This can be done iteratively to obtain a consistent set of values, and the result of the fitting was $w = 0.493 \pm 0.015$ and $l_{p,0} = 37.0 \pm 5.6$ nm when excluding the two lowest concentrations of added salt because of the large uncertainties (see section 4.1). In the logarithmic plot, the highest salt concentration is also excluded because the persistence length at 3 M is 34.4 nm, which is less than 37.0 nm, and the difference is negative. The fitted value of A is 2.94 ± 0.12.

The two resulting plots with the regression lines are shown in Figure 6. It is interesting to note that the value at $C_s = 10^{-5}$ M is quite close to the line, although it was not used in the

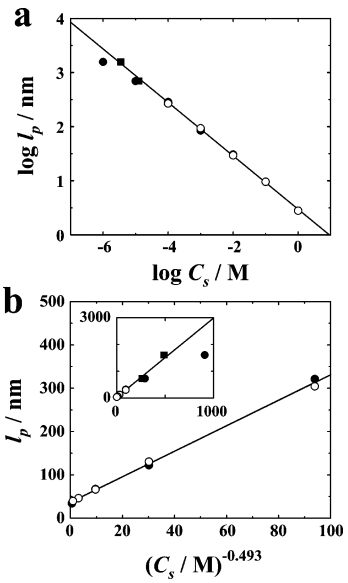

Figure 6. Persistence length as a function of the concentration of added 1:1 salt (a) as a log−log plot and (b) as a power law to determine the parameters of eq 8. The graphs show the results for the final choice of $l_{p,0} = 37.0$ nm and $w = 0.493$ with the solid lines showing the result of the linear regression for $C_s = 10^{-4}$−1 M and $C_s = 10^{-4}$−3 M for the logarithmic (a) and power-law (b) plots, respectively. The inset in (b) is the same graph, but with extended axes to include the points omitted in the fitting. YOYO-1 data are represented by filled circles and DAPI data with open circles, while filled squares are values shifted to correspond to the ionic strength assuming a pH of 5.6.

fitting. The "correction" assuming a pH of 5.6 brings it even closer, while at $C_s = 10^{-6}$ M, the "correction" overshoots. However, it shows that with an adjusted interpretation of ionic strength the power-law behavior seen at higher salt concentrations may actually be valid also at the lowest ionic strengths, although the general uncertainty and the risk of local DNA denaturation (see section 4.1) make this a somewhat shaky statement.

The power $w = 0.493$ shows that electrostatic persistence length is more or less inversely proportional to the square root of the salt concentration, which is equivalent to a linear dependence on the screening length. This is the expected behavior for a flexible polyelectrolyte in a regime where excluded-volume interactions are important.[17,30,31] Since the contour length of T4 DNA is very long compared to the persistence length, this is indeed the behavior that the molecule would be expected to have. Also looking at Figure 1, it is clear that excluded-volume interactions should have a significant effect, even at the lowest concentration of added salt.

The figure also illustrates another important point. A difference between a wormlike chain and a charged chain is that the latter has different behavior on different length scales, where the short-range behavior represents a more flexible chain than the long-range, as has been demonstrated in simulation studies,[15−17] and can also be seen in Table 2 as smaller bond angles for the charged chains than the freely rotating chains at the same degree of global extension or shape factor. It is one of the fundamental reasons why different definitions of persistence lengths give different results for self-interacting chains. The separation of length scales is also the basis of the blob model,[46,59] which assumes that the chain is unperturbed at short range, while electrostatic effects are seen in the long-range behavior as a rescaled chain. In Figure 1, the image taken at 1 μM added NaCl clearly shows the difference in local and global behavior. While there on average may be a persistent direction over large parts of the molecule, there are many twists and turns on a shorter length scale.

The value for the intrinsic persistence length, $l_{p,0} = 37.0$ nm, is significantly lower than the commonly quoted value of 50 nm.[1−4] On the other hand, our value is in the range found by Porschke[60] and also in agreement with results of Borochov, Eisenberg, and Kam.[32,34] In the case of the latter, the low value has been attributed to an excluded-volume treatment,[1] but preliminary studies of our own indicate that the results cannot be dismissed that easily. This will be discussed in more detail in a future communication.

We have ruled out the possibility that the dye molecules are responsible for a change in DNA stiffness leading to the deviation of $l_{p,0}$ from the established value. We base this on the observations of Matsuzawa and Yoshikawa (MY).[51] They investigated the binding of DAPI to T4 DNA and its influence on the persistence length by changing the bulk concentration of the dye. DAPI was the dye used at the high salt concentrations where we observed somewhat short persistence lengths. Using the results of the binding studies of MY, we calculate the amount of bound DAPI to 0.017 molecule per nucleotide. At this value, the persistence length curve obtained by MY shows a slight increase rather than a decrease, as can be expected from a groove binder when electrostatic interactions can be neglected. YOYO-1, used at low salt concentrations, does affect the chain and extends the contour length to some degree, but this is compensated for in the calculation of projection length by the measured contour length. The effects of YOYO-1 could in principle influence the power law, but the fitting only includes YOYO-1 data at salt concentrations where the results can be compared to DAPI measurements and the two sets are consistent. Thus, we do not expect the dyes to have any impact on the general conclusions. The fact that similarly low values of $l_{p,0}$ have also been obtained with other techniques lends further support to the idea that the dye molecules are not the cause.

5. Conclusions

Fluorescence microscopy measurements were performed on individual giant double-stranded T4 DNA molecules at a wide range of added NaCl, 1×10^{-6}−3 M. To make the results generally comparable to theory and to other experiments, a connection had to be made between the measured long-axis length L_{long} and a more common property. Simulations showed that L_{long} is correlated to the radius of gyration R_G with an almost constant ratio $R_G/L_{long} \approx 0.4$ for models ranging from freely jointed chains to rigid rods. The radius of gyration, in turn, can be expressed as the persistence length of an effective wormlike chain, even if the chain is not wormlike. Defined this way, the resulting persistence length is a projection length.

Under the assumptions that the electrostatic contribution to the persistence length is additive and that all electrostatic effects, including excluded-volume effects, can be described by a simple power law in the salt concentration, we find an intrinsic persistence length of 37.0 nm and an electrostatic persistence length almost inversely proportional the square root of to the salt concentration ($l_{p,0} \sim C_s^{-0.493}$), which is the same as linearly dependent on the screening length. This intrinsic persistence length is significantly shorter than the usually quoted value of 50 nm, but as an experimental result, this is not unique. The linear dependence on the screening length is consistent with the behavior of a polyelectrolyte influenced by excluded-volume effects, i.e., occasional interactions between distant parts of the chain. Since T4 DNA is very long, it is reasonable that such effects are important, and the fluorescence images also confirm

that the overall flexibility is high enough, even at the lowest salt concentration.

Acknowledgment. The contribution by M.U. was supported by the JSPS fellowship program. M.U. also thanks Rita Dias and Mónica Rosa for helpful hints and discussions.

References and Notes

(1) Hagerman, P. J. *Annu. Rev. Biophys. Biophys. Chem.* **1988**, *17*, 265−286.
(2) Taylor, W. H.; Hagerman, P. J. *J. Mol. Biol.* **1990**, *212*, 363−376.
(3) Sobel, E. S.; Harpst, J. A. *Biopolymers* **1991**, *31*, 1559−1564.
(4) Bustamante, C.; Marko, J. F.; Siggia, E. D.; Smith, S. *Science* **1994**, *265*, 1599−1600.
(5) Yoshikawa, K.; Matsuzawa, Y. *Physica D* **1995**, *84*, 220−227.
(6) Mel′nikov, S. M.; Sergeyev, V. G.; Yoshikawa, K. *J. Am. Chem. Soc.* **1995**, *117*, 9951−9956.
(7) Yoshikawa, K.; Kidoaki, S.; Takahashi, M.; Vasilevskaya, V. V.; Khokhlov, A. R. *Ber. Bunsen-Ges. Phys. Chem.* **1996**, *100*, 876−880.
(8) Takahashi, M.; Yoshikawa, K.; Vasilevskaya, V. V.; Khokhlov, A. R. *J. Phys. Chem. B* **1997**, *101*, 9396−9401.
(9) Yamasaki, Y.; Yoshikawa, K. *J. Am. Chem. Soc.* **1997**, *119*, 10573−10578.
(10) Mel'nikov, S. M.; Sergeyev, V. G.; Mel'nikova, Y. S.; Yoshikawa, K. *J. Chem. Soc., Faraday Trans.* **1997**, *93*, 283−288.
(11) Mel'nikov, S. M.; Yoshikawa, K. *Biochem. Biophys. Res. Commun.* **1997**, *230*, 514−517.
(12) Ullner, M. In *Handbook of Polyelectrolytes and Their Applications*; Tripathy, S. K., Kumar, J., Nalwa, H. S., Eds.; American Scientific Publishers: Los Angeles, 2002; Vol. 3, pp 271−308.
(13) Odijk, T. *J. Polym. Sci., Polym. Phys. Ed.* **1977**, *15*, 477−483.
(14) Skolnick, J.; Fixman, M. *Macromolecules* **1977**, *10*, 944−948.
(15) Ullner, M.; Woodward, C. E. *Macromolecules* **2002**, *35*, 1437−1445.
(16) Ullner, M.; Jönsson, B.; Peterson, C.; Sommelius, O.; Söderberg, B. *J. Chem. Phys.* **1997**, *107*, 1279−1287.
(17) Ullner, M. *J. Phys. Chem. B* **2003**, *107*, 8097−8110.
(18) Maret, G.; Weill, G. *Biopolymers* **1983**, *22*, 2727−2744.
(19) Mattoussi, H.; O'Donohue, S.; Karasz, F. E. *Macromolecules* **1992**, *25*, 743−749.
(20) Baumann, C. G.; Smith, S. B.; Bloomfield, V. A.; Bustamante, C. *Proc. Natl. Acad. Sci. U.S.A.* **1997**, *94*, 6185−6190.
(21) Tricot, M. *Macromolecules* **1984**, *17*, 1698−1704.
(22) Ghosh, S.; Li, X.; Reed, C. E.; Reed, W. F. *Biopolymers* **1990**, *30*, 1101−1112.
(23) Reed, W. F.; Ghosh, S.; Medjahdi, G.; Francois, J. *Macromolecules* **1991**, *24*, 6189−6198.
(24) Degiorgio, V.; Mantegazza, F.; Piazza, R. *Europhys. Lett.* **1991**, *15*, 75−80.
(25) Sorci, G. A.; Reed, W. F. *Macromolecules* **2002**, *35*, 5218−5227.
(26) Sorci, G. A.; Reed, W. F. *Macromolecules* **2004**, *37*, 554−565.
(27) Reed, C. E.; Reed, W. F. *J. Chem. Phys.* **1991**, *94*, 8479−8486.
(28) Barrat, J.-L.; Boyer, D. *J. Phys. II* **1993**, *3*, 343−356.
(29) Seidel, C. *Ber. Bunsen-Ges. Phys. Chem.* **1996**, *100*, 757−763.
(30) Everaers, R.; Milchev, A.; Yamakov, V. *Eur. Phys. J. E* **2002**, *8*, 3−14.
(31) Nguyen, T. T.; Shklovskii, B. I. *Phys. Rev. E* **2002**, *66*, 021801.
(32) Borochov, N.; Eisenberg, H.; Kam, Z. *Biopolymers* **1981**, *20*, 231−235.
(33) Sharp, P.; Bloomfield, V. A. *Biopolymers* **1968**, *6*, 1201−1211.
(34) Kam, Z.; Borochov, N.; Eisenberg, H. *Biopolymers* **1981**, *20*, 2671−2690.
(35) Fouissac, E.; Milas, M.; Rinaudo, M.; Borsali, R. *Macromolecules* **1992**, *25*, 5613−5617.
(36) Odijk, T.; Houwaart, A. C. *J. Polym. Sci., Polym. Phys. Ed.* **1978**, *16*, 627−639.
(37) Reed, C. E.; Reed, W. F. *J. Chem. Phys.* **1990**, *92*, 6916−6926.
(38) Reed, C. E.; Reed, W. F. *J. Chem. Phys.* **1992**, *97*, 7766−7776.
(39) Barrat, J.-L.; Joanny, J.-F. *Europhys. Lett.* **1993**, *24*, 333−338.
(40) Beer, M.; Schmidt, M.; Muthukumar, M. *Macromolecules* **1997**, *30*, 8375−8385.
(41) Muthukumar, M. *J. Chem. Phys.* **1987**, *86*, 7230−7235.
(42) Muthukumar, M. *J. Chem. Phys.* **1996**, *105*, 5183−5199.
(43) Kuhn, W.; Künzle, O.; Katchalsky, A. *Helv. Chim. Acta* **1948**, *31*, 1994−2037.
(44) Katchalsky, A.; Künzle, O.; Kuhn, W. *J. Polym. Sci.* **1950**, *5*, 283−300.
(45) Fisher, M. E. *J. Phys. Soc. Jpn., Suppl.* **1969**, *26*, 44−45.
(46) de Gennes, P. G.; Pincus, P.; Velasco, R. M.; Brochard, F. *J. Phys. (Paris)* **1976**, *37*, 1461−1473.
(47) Manghi, M.; Netz, R. R. *Eur. Phys. J. E* **2004**, *14*, 67−77.
(48) Metropolis, N. A.; Rosenbluth, A. W.; Rosenbluth, M. N.; Teller, A.; Teller, E. *J. Chem. Phys.* **1953**, *21*, 1087−1097.
(49) Lal, M. *Mol. Phys.* **1969**, *17*, 57−64.
(50) Madras, N.; Sokal, A. D. *J. Stat. Phys.* **1988**, *50*, 109−186.
(51) Matsuzawa, Y.; Yoshikawa, K. *Nucleosides Nucleotides* **1994**, *13*, 1415−1423.
(52) Arnott, S.; Hukins, D. W. L. *J. Mol. Biol.* **1973**, *81*, 93−105.
(53) Arnott, S.; Chandrasekaran, R.; Birdsall, D. L.; Leslie, A. G. W.; Ratliff, R. L. *Nature (London)* **1980**, *283*, 743−745.
(54) Neidle, S. *DNA Structure and Recognition*; Oxford University Press: Oxford, 1994.
(55) Inman, R. B.; Jordan, D. O. *Biochim. Biophys. Acta* **1960**, *42*, 421−426.
(56) Inman, R. B.; Jordan, D. O. *Biochim. Biophys. Acta* **1960**, *42*, 427−434.
(57) Korolev, N. I.; Vlasov, A. P.; Kuznetzov, I. A. *Biopolymers* **1994**, *34*, 1275−1290.
(58) Rosa, M.; Dias, R.; Miguel, M. G.; Lindman, B. *Biomacromolecules* **2005**, *6*, 2164−2171.
(59) Khokhlov, A. R.; Khachaturian, K. A. *Polymer* **1982**, *23*, 1742−1750.
(60) Porschke, D. *Biophys. Chem.* **1991**, *40*, 169−179.

MA060669B